$(NH_4)_2Te_2WO_8$: A New Polar Oxide with Second-Harmonic Generating, Ferroelectric, and Pyroelectric Properties

Jun-Ho Kim, Jaewook Baek, and P. Shiv Halasyamani*

Department of Chemistry and Center for Materials Chemistry, University of Houston, 136 Fleming Building, Houston, Texas 77204-5003

Received July 19, 2007. Revised Manuscript Received September 10, 2007

A new polar ammonium tungsten tellurite, $(NH_4)_2Te_2WO_8$, has been synthesized and structurally characterized. The material was synthesized hydrothermally, using NH_4OH, WO_3, and TeO_2 as reagents, and structurally characterized by single-crystal X-ray diffraction. $(NH_4)_2Te_2WO_8$ crystallizes in the noncentrosymmetric (NCS) polar monoclinic space group $P2_1$ (No. 4) with $a = 6.9716(9)$ Å, $b = 7.0279(9)$ Å, $c = 9.4593(13)$ Å, and $\beta = 99.188(2)°$. The material exhibits a two-dimensional structure consisting of WO_6 octahedra connected to TeO_4 polyhedra. Both the W^{6+} and the Te^{4+} cations are in asymmetric coordination environments attributable to second-order Jahn−Teller (SOJT) effects. $(NH_4)_2Te_2WO_8$ is NCS; thus second-harmonic generation (SHG) measurements were performed. SHG experiments, using 1064 nm radiation, revealed an efficiency of approximately 250 × α-SiO_2. As $(NH_4)_2Te_2WO_8$ is also polar, ferroelectric and pyroelectric measurements were performed. A ferroelectric hysteresis loop (polarization vs electric field) was observed, indicating the dipole moment in $(NH_4)_2Te_2WO_8$ is "switchable". A spontaneous polarization (P_s) of 0.19 $\mu C/cm^2$ was measured. In addition, the pyroelectric coefficient (total effect), p, was determined to be -0.22 $\mu C/m^2 \cdot K$ at 50 °C.

Introduction

Polarity, the presence of a dipole moment, is rather common in molecular systems, for example, H_2O, NH_3, HCl, etc. In such molecular systems, the concept of a dipole moment is rather straightforward. In compounds that exhibit extended structures, solid-state materials, the concept of polarity is a bit more complicated. For a solid-state material to be considered polar, the compound must crystallize in one of 10 crystal classes, 1, 2, 3, 4, 6, *m*, *mm*2, 3*m*, 4*mm*, or 6*mm*.[1] In addition, within each of these crystal classes there are specifically defined polar directions.[1] Interest in polarity and polar materials, in solid-state compounds, stems from two technologically important properties, pyroelectricity and ferroelectricity.[2,3] For both phenomena to occur, the material in question must be polar. With pyroelectricity, a change in the magnitude of the polarization, dipole moment, with respect to temperature is observed, whereas with ferroelectricity the dipole moment may be switched in the presence of an external electric field. For pyroelectrics, this dipole moment "switchability" does not occur. Thus, all ferroelectrics are pyroelectrics, but the converse is not true. Both pyroelectrics and ferroelectrics have important technological functions. Pyroelectrics are used as thermal detectors, whereas ferroelectrics find uses in computer memories.[2,3]

Although polarity and polar materials are clearly important, the question remains of how to synthesize new polar materials. To answer this question, we have synthesized several polar materials containing d^0 transition metal cations (Ti^{4+}, Nb^{5+}, W^{6+}, etc.) and lone-pair cations (Sb^{3+}, Se^{4+}, Te^{4+}, etc.).[4−9] In oxide coordination environments, both groups of cations are in asymmetric coordination environments attributable to second-order Jahn−Teller (SOJT) effects.[10−16] With the d^0 cation, an out-of-center displacement is observed,[17] whereas with the lone-pair cation a nonbonded electron pair is found.[18] In both instances, the local site symmetry of the cation is changed from centrosymmetric to noncentrosymmetric and polar. Often the cations exhibit polar local site symmetries of 3*m* (C_{3v}) or 4*mm* (C_{4v}). Also, of the 91 structurally well-characterized oxides that contain a d^0 transition metal and a lone-pair cation, 36, nearly 40%, are

* To whom correspondence should be addressed. Phone: (713) 743-3278. Fax: (713) 743-0796. E-mail: psh@uh.edu.

(1) Hahn, T. *International Tables for Crystallography, Volume A, Space Group Symmetry*; Kluwer Academic: Dordrecht, Holland, 2006; Vol. A.
(2) Lang, S. B. *Phys. Today* **2005**, *58*, 31.
(3) Auciello, O.; Scott, J. F.; Ramesh, R. *Phys. Today* **1998**, *51*, 22.
(4) Ok, K. M.; Bhuvanesh, N. S. P.; Halasyamani, P. S. *J. Solid State Chem.* **2001**, *161*, 57.
(5) Goodey, J.; Broussard, J.; Halasyamani, P. S. *Chem. Mater.* **2002**, *14*, 3174.
(6) Goodey, J.; Ok, K. M.; Broussard, J.; Hofmann, C.; Escobedo, F. V.; Halasyamani, P. S. *J. Solid State Chem.* **2003**, *175*, 3.
(7) Ra, H. S.; Ok, K. M.; Halasyamani, P. S. *J. Am. Chem. Soc.* **2003**, *125*, 7764.
(8) Chi, E. O.; Gandini, A.; Ok, K. M.; Zhang, L.; Halasyamani, P. S. *Chem. Mater.* **2004**, *16*, 3616.
(9) Chi, E. O.; Ok, K. M.; Porter, Y.; Halasyamani, P. S. *Chem. Mater.* **2006**, *18*, 2070.
(10) Opik, U.; Pryce, M. H. L. *Proc. R. Soc. London, Ser. A* **1957**, *238*, 425.
(11) Bader, R. F. W. *Mol. Phys.* **1960**, *3*, 137.
(12) Bader, R. F. W. *Can. J. Chem.* **1962**, *40*, 1164.
(13) Pearson, R. G. *J. Am. Chem. Soc.* **1969**, *91*, 4947.
(14) Pearson, R. G. *J. Mol. Struct. (THEOCHEM)* **1983**, *103*, 25.
(15) Wheeler, R. A.; Whangbo, M. H.; Hughbanks, T.; Hoffmann, R.; Burdett, J. K.; Albright, T. A. *J. Am. Chem. Soc.* **1986**, *108*, 2222.
(16) Kunz, M.; Brown, I. D. *J. Solid State Chem.* **1995**, *115*, 395.
(17) Goodenough, J. B. *Annu. Rev. Mater. Sci.* **1998**, *28*, 1.
(18) Stoltzfus, M. W.; Woodward, P.; Seshadri, R.; Park, J.-H.; Bursten, B. *Inorg. Chem.* **2007**, *46*, 3839.

10.1021/cm7019334 CCC: $37.00
Published on Web 10/09/2007

polar. This indicates that the local polar environment of the cations is retained in the solid-state structure.

One set of SOJT-effect distorted cations that we have investigated is Te^{4+} and W^{6+}. Interestingly, of the eight reported oxides that contain Te^{4+} and W^{6+}, *$Na_2TeW_2O_9$* (*Ia*),[5] $K_2TeW_3O_{12}$ (*P*$2_1/n$),[6] *$Rb_2TeW_3O_{12}$* (*P*6_3),[6] *$Cs_2TeW_3O_{12}$* (*P*6_3),[6] $Na_2TeW_4O_{12}$ (*C*2/*c*),[19] *$BaTeW_2O_9$* (*P*2),[7] $BiTeW_2O_{10}$ (*C*2/*c*),[20] and $Bi_2Te_2W_3O_{16}$ (*C*2/*c*),[21] four, 50%, are polar. These are shown in italics. We have continued our investigation of materials containing these cations. In this Article, we report on the synthesis and characterization of a new polar oxide, $(NH_4)_2Te_2WO_8$.

Experimental Section

Reagents. TeO_2 (99% Aldrich), WO_3 (99% Aldrich), and NH_4-OH (30% EM Science) were used as received.

Syntheses. Single crystals of $(NH_4)_2Te_2WO_8$ were synthesized hydrothermally from a solution of WO_3 (0.232 g, 1 mmol), TeO_2 (0.239 g, 1.5 mmol), and 2 mL of NH_4OH. The mixture was put in a 23 mL Teflon lined autoclave. The autoclave was closed, heated to 230 °C for 2 days, cooled to 100 °C at 6 °C h^{-1}, and then cooled to room temperature within 2 h. Pale yellow hexagonal plate-shaped crystals, subsequently shown to be $(NH_4)_2Te_2WO_8$, were obtained after filtration in 80% yield based on TeO_2.

Structure Determination. The structure of $(NH_4)_2Te_2WO_8$ was determined by standard crystallographic methods. A pale yellow hexagonal block ($0.02 \times 0.02 \times 0.08$ mm^3) was used for single-crystal measurement. Room-temperature intensity data were collected on a Siemens SMART diffractometer equipped with a 1 K CCD area detector using graphite monochromated Mo Kα radiation. A hemisphere of data was collected using a narrow-frame method with scan widths of 0.30° in omega and an exposure time of 30 s $frame^{-1}$. The first 50 frames were remeasured at the end of the data collection to monitor instrument and crystal stabilities. The maximum correction applied to the intensities was <1%. The data were integrated using the Siemens SAINT program,[22] with the intensities corrected for Lorentz polarization, air absorption, and absorption attributable to the variation in the path length through the detector faceplate. Ψ-Scans were used for the absorption correction on the hemisphere of data. The data were solved and refined using SHELXS-97 and SHELXL-97, respectively.[23,24] All atoms were refined with anisotropic thermal parameters and converged for $I > 2\sigma(I)$. All calculations were performed using the WinGX-98 crystallographic software package.[25] Crystallographic data, atomic coordinates, and selected bond distances for $(NH_4)_2Te_2WO_8$ are given in Tables 1−3 with additional details found in the Supporting Information.

Thermogravimetric Analysis. Thermogravimetric analysis was carried out on a TGA 2950 thermogravimetric analyzer (TA Instruments). The sample was placed in a platinum crucible and heated at a rate of 10 °C min^{-1} from room temperature to 900 °C under flowing nitrogen gas.

Table 1. Crystallographic Data for $(NH_4)_2Te_2WO_8$

formula	$(NH_4)_2Te_2WO_8$
fw	603.13
T (K)	296.0(2)
λ (Å)	0.71073
crystal dimensions (mm^3)	$0.02 \times 0.02 \times 0.08$
color, habit	pale yellow, hexagonal plate
crystal system	monoclinic
space group	$P2_1$ (No. 4)
a (Å)	6.9716(9)
b (Å)	7.0279(9)
c (Å)	9.4593(13)
β (deg)	99.188(2)
V ($Å^3$)	457.52(10)
Z	2
ρ_{calcd} (g/cm^3)	4.378
μ (mm^{-1})	18.893
$2\theta_{max}$ (deg)	56.66
absorption correction	Ψ-scan
R(int)	0.0373
Flack parameter	0.062(11)
GOF	0.922
extinction coefficient	0.0028(2)
$R(F)^a$	0.0318
$R_w(F_o^2)^b$	0.0597

[a] $R(F) = \sum||F_o| - |F_c||/\sum|F_o||$. [b] $R_w(F_o^2) = \{\sum[w(F_o^2 - F_c^2)^2]/\sum[w(F_o^2)^2]\}^{1/2}$.

Table 2. Atomic Coordinates for $(NH_4)_2Te_2WO_8$

atom	x	y	z	$U_{eq}{}^a$/$Å^2$
Te(1)	−0.0357(1)	0.2760(1)	1.0019(1)	0.012(1)
Te(2)	0.0523(1)	0.0145(1)	1.3586(1)	0.014(1)
W(1)	0.1685(1)	0.0747(1)	0.7407(1)	0.012(1)
O(1)	0.3107(14)	0.2405(12)	0.6699(11)	0.024(2)
O(2)	0.3387(13)	−0.0877(12)	0.8292(10)	0.022(2)
O(3)	0.0791(14)	−0.0649(11)	0.5798(10)	0.018(2)
O(4)	0.1977(12)	0.2345(11)	0.9302(9)	0.013(2)
O(5)	0.0734(12)	−0.2437(11)	1.3125(9)	0.014(2)
O(6)	0.0502(12)	0.4463(11)	1.1534(9)	0.014(2)
O(7)	0.0199(13)	0.0566(13)	1.1307(8)	0.022(2)
O(8)	0.3093(12)	0.0806(15)	1.3772(9)	0.024(2)
N(1)	0.4977(15)	−0.4540(15)	0.8629(11)	0.020(2)
N(2)	0.6160(16)	−0.198(17)	1.5959(13)	0.028(3)

[a] U_{eq} is defined as one-third of the trace of the orthogonalized U_{ij} tensor.

Table 3. Selected Bond Distances (Å) for $(NH_4)_2Te_2WO_8$

W(1)−O(1)	1.733(9)	Te(1)−O(4)	1.882(8)
W(1)−O(2)	1.759(9)	Te(1)−O(6)	1.890(8)
W(1)−O(3)	1.834(9)	Te(1)−O(7)	1.965(9)
W(1)−O(4)	2.097(8)	Te(1)−O(7)	2.349(9)
W(1)−O(5)	2.110(8)		
W(1)−O(6)	2.151(8)	Te(2)−O(8)	1.832(8)
		Te(2)−O(5)	1.878(7)
		Te(2)−O(3)	2.145(9)
		Te(2)−O(7)	2.152(8)

Powder X-ray Diffraction. The X-ray powder diffraction data were collected on a Scintag XDS2000 diffractometer at room temperature (Cu Kα radiation, $\theta-\theta$ mode, flat plate geometry) equipped with Peltier germanium solid-state detector in the 2θ range 5−60° with a step size of 0.02° and a step time of 1 s.

Infrared, Raman, and UV−Vis Diffuse Reflectance Spectroscopy. The infrared spectra were recorded on a Matteson FT-IR 5000 spectrometer. The sample was mixed with dry KBr and pressed into a pellet. The Raman spectra were recorded at room temperature on a Digilab FTS 7000 spectrometer equipped with a HgCdTe detector with the powder sample placed in a capillary tube. Excitation was provided by a Nd:YAG laser at a wavelength of 1064 nm, and the output laser power was 500 mW. The spectral

(19) Balraj, V.; Vidyasagar, K. *Inorg. Chem.* **1999**, *38*, 5809.
(20) Champarnaud-Mesjard, J. C.; Frit, B.; Chagraoui, A.; Tairi, A. *Z. Anorg. Allg. Chem.* **1996**, *622*, 248.
(21) Champarnaud-Mesjard, J. C.; Frit, B.; Chagraoui, A.; Tairi, A. *J. Solid State Chem.* **1996**, *127*, 248.
(22) *SAINT, Program for Area Detector Absorption Correction*, 4.05; Siemens Analytical X-ray Systems, Inc.: Madison, WI, 1995.
(23) Sheldrick, G. M. *SHELXS-97 - A program for automatic solution of crystal structures*; University of Goettingen: Goettingen, Germany, 1997.
(24) Sheldrick, G. M. *SHELXL-97 - A program for crystal structure refinement*; University of Goettingen: Goettingen, 1997.
(25) Farrugia, L. J. *J. Appl. Crystallogr.* **1999**, *32*, 837.

resolution was about 4 cm^{-1}, and 256 scans were collected. UV−vis diffuse reflectance spectrum for $(NH_4)_2Te_2WO_8$ was collected with a Varian Cary 500 scan UV−vis−NIR spectrophotometer over the spectral range 200−2500 nm at room temperature. Poly(tetrafluoroethylene) was used as a reference material. Reflectance spectra were converted to absorbance with the Kubelka−Munk equation.[26]

Second-Order Nonlinear Optical Measurements. Powder SHG measurements on polycrystalline $(NH_4)_2Te_2WO_8$ were performed on a modified Kurtz-NLO system using 1064 nm radiation. A detailed description of the equipment and methodology used has been published.[27] The SHG efficiency has been shown to depend strongly on particle size; thus the polycrystalline samples were ground and sieved into distinct particle size ranges.[28] To make relevant comparisons with known SHG materials, we also ground and sieved crystalline SiO_2 and $LiNbO_3$ into the same particle size ranges.

Polarization Measurements. The polarization was measured on a Radiant Technologies RT66A ferroelectric test system with a TREK high-voltage amplifier between room temperature and 230 °C in a Delta 9023 environmental test chamber. The unclamped pyroelectric coefficient, defined as d*P*/d*T* (change in polarization with respect to the change in temperature), was determined by measuring the polarization as a function of temperature. The sample was a sintered 1/2 in. diameter disk (approximately 90% dense) and approximately 0.5 mm thick. Silver paste was applied to both sides. The polarization was measured statically from room temperature to 230 °C in 10 °C increments, with an electric field of 46 kV/cm. The temperature was allowed to stabilize before the polarization was measured.

Piezoelectric Measurements. Both direct and converse piezoelectric measurements were attempted. Attributable to the low decomposition temperature of the material, ∼240 °C, we were unable to sinter a dense enough pellet for the measurements.

Results and Discussion

$(NH_4)_2Te_2WO_8$ exhibits a two-dimensional structural topology, consisting of WO_6 octahedra connected to TeO_4 polyhedra (see Figure 1). The layers of these WO_6 and TeO_4 polyhedra are separated by the NH_4^+ cations (see Figure 2). Each WO_6 octahedron is surrounded by four TeO_4 polyhedra. In connectivity terms, the structure may be written as $\{[WO_{2/1}O_{4/2}]^{2-}[TeO_{2/2}O_{2/3}]^{+2/3}[TeO_{1/1}O_{2/2}O_{1/3}]^{-2/3}\}^{2-}$ with charge balance maintained by the two NH_4^+ cations. The W−O and Te−O bond distances range from 1.733(9) to 2.151(8) Å and 1.832(8) to 2.349(9) Å, respectively. Bond valence calculations[29,30] resulted in values of 6.17 for W^{6+} and 3.96 and 4.05 for Te^{4+}. Both W^{6+} and Te^{4+} are in asymmetric coordination environments attributable to second-order Jahn−Teller (SOJT) effects.[10−16] With the unique W^{6+} cation, this effect is manifested structurally as an out-of-center distortion toward a face of the WO_6 octahedron (see Figure 3). This face, or C_3, distortion is the most commonly observed for octahedrally coordinated W^{6+} cations.[31] In addition, using continuous symmetry measures,[32−35] we were able to calculate the magnitude of the out-of-center distortion. For the unique W^{6+} cation, this value is 0.103 $Å^2$, which is larger than the 0.062 $Å^2$ average reported earlier for octahedrally coordinated W^{6+} cations.[36] With the Te^{4+} cations, a stereo-active lone-pair is observed that results in an asymmetric coordination environment (see Figure 3). We can also calculate the dipole moment of the WO_6 and TeO_4 polyhedra using a methodology described earlier.[37−39] The

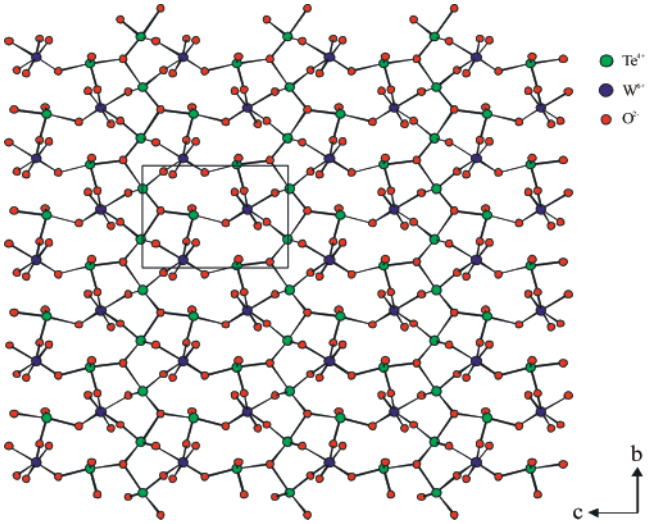

Figure 1. Ball-and-stick representation in the *bc*-plane of $(NH_4)_2Te_2WO_8$ is shown. The NH_4^+ cations have been removed for clarity.

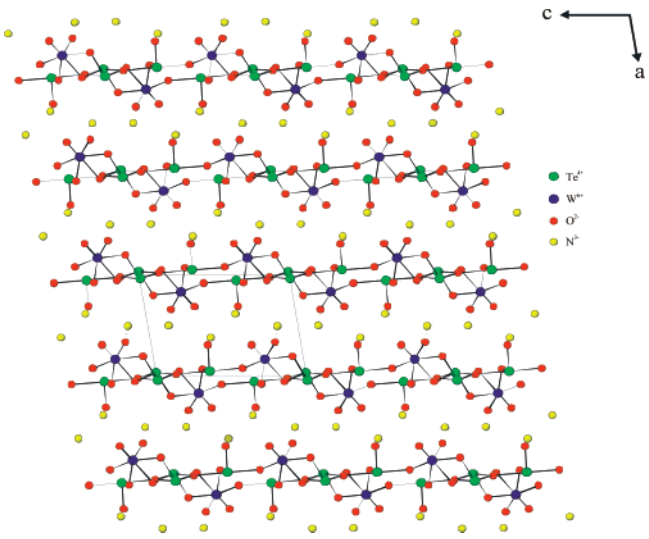

Figure 2. Ball-and-stick representation in the *ac*-plane of $(NH_4)_2Te_2WO_8$ is shown. The NH_4^+ cations interact with the layers through N−H− − −O hydrogen bonding (shown as dashed lines).

(26) Kubelka, P.; Munk, F. *Z. Tech. Phys.* **1931**, *12*, 593.
(27) Ok, K. M.; Chi, E. O.; Halasyamani, P. S. *Chem. Soc. Rev.* **2006**, *35*, 710.
(28) Kurtz, S. K.; Perry, T. T. *J. Appl. Phys.* **1968**, *39*, 3798.
(29) Brown, I. D.; Altermatt, D. *Acta Crystallogr., Sect. B* **1985**, *41*, 244.
(30) Brese, N. E.; Okeeffe, M. *Acta Crystallogr., Sect. B* **1991**, *47*, 192.
(31) Halasyamani, P. S. *Chem. Mater.* **2004**, *16*, 3586.
(32) Zabrodsky, H.; Peleg, S.; Avnir, D. *J. Am. Chem. Soc.* **1992**, *114*, 7843.
(33) Alvarez, S.; Avnir, D.; Llunell, M.; Pinsky, M. *New J. Chem.* **2002**, *26*, 996.
(34) Alvarez, S.; Alemany, P.; Avnir, D. *Chem. Soc. Rev.* **2005**, *34*, 313.
(35) Llunell, M.; Casanova, D.; Cirera, J.; Bofill, J. M.; Alemany, P.; Alvarez, S.; Pinsky, M.; Avnir, D. *Shape Program, Version 1.1b*; University of Barcelona: Barcelona, Spain, 2004.
(36) Ok, K. M.; Halasyamani, P. S.; Casanova, D.; Llunell, M.; Alemany, P.; Alvarez, S. *Chem. Mater.* **2006**, *18*, 3176.
(37) Maggard, P. A.; Nault, T. S.; Stern, C. L.; Poeppelmeier, K. R. *J. Solid State Chem.* **2003**, *175*, 27.
(38) Izumi, H. K.; Kirsch, J. E.; Stern, C. L.; Poeppelmeier, K. R. *Inorg. Chem.* **2005**, *44*, 884.
(39) Ok, K. M.; Halasyamani, P. S. *Inorg. Chem.* **2004**, *43*, 4248.

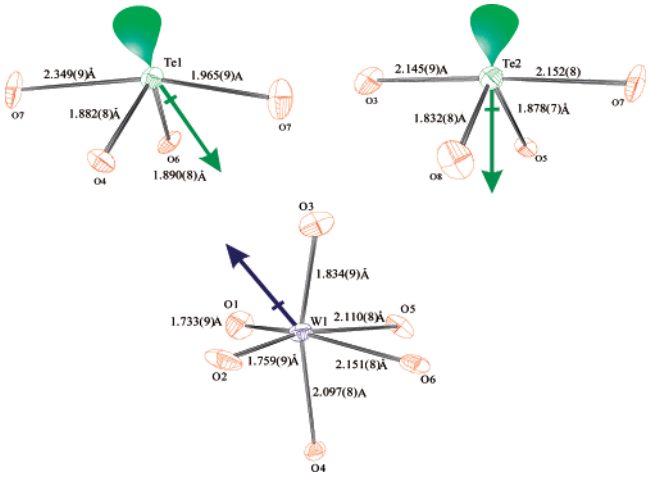

Figure 3. ORTEP (50% probability ellipsoids) drawings of the TeO_4 and WO_6 polyhedra are shown. The green and blue arrows indicate the approximate direction of the dipole moments for TeO_4 and WO_6 polyhedra, respectively.

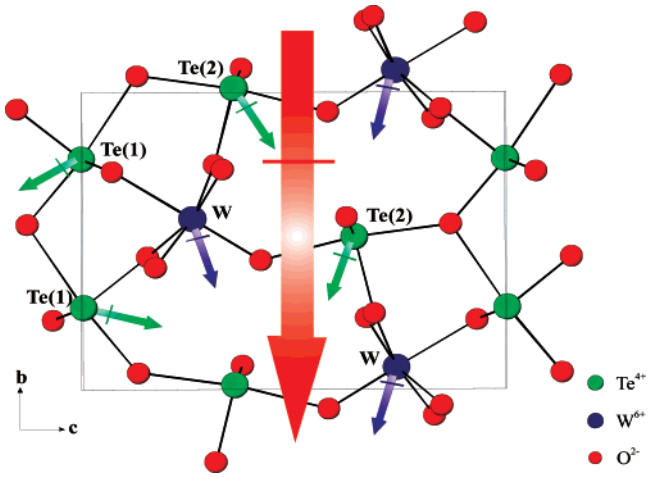

Figure 4. Ball-and-stick representation of the TeO_4 and WO_6 polyhedra is shown. The direction of the local dipole moments for each polyhedra is shown in green (TeO_4) and blue (WO_6). The large red arrow represents the direction of the net dipole moment for $(NH_4)_2Te_2WO_8$.

calculations resulted in values of 1.55D for the WO_6 octahedron, and 10.40 and 8.51D for the two unique TeO_4 polyhedra. These values are consistent with those reported earlier.[39]

The infrared and Raman spectra of $(NH_4)_2Te_2WO_8$ revealed Te−O, W−O, and W−O−Te vibrations between 600 and 950 cm^{-1} (see Table 4). In both the IR and the Raman spectra, peaks between 800 and 950 cm^{-1} and 670 and 800 cm^{-1} can be attributed to W−O and Te−O stretches, respectively. W−O−Te vibrations are observed in the IR and Raman spectra between 600 and 660 cm^{-1}. The assignments are consistent with those previously reported.[6,19,40−43] The thermal behavior of $(NH_4)_2Te_2WO_8$ was investigated using thermogravimetric analysis. An initial weight loss starting around 240 °C is consistent with the loss of 2 mol of NH_3 (obs., 5.58%; calc., 5.65%). Above this temperature, the material decomposes to the binary oxides, WO_3 and TeO_2. Around 720 °C, TeO_2 is lost and only WO_3 remains. The TGA curve is available in the Supporting Information.

$(NH_4)_2Te_2WO_8$ crystallizes in a noncentrosymmetric space group, $P2_1$, indicating the material should be SHG active. We sieved the polycrystalline powder into various particle sizes, 20−120 μm, and measured the SHG efficiency as a function of particle size. We determined that $(NH_4)_2Te_2WO_8$ is phase-matchable with a SHG efficiency of ~250 × α-SiO_2. This indicates that $(NH_4)_2Te_2WO_8$ falls into class A of SHG materials as defined by Kurtz and Perry.[28] Once the phase-matching behavior has been determined and the SHG efficiency measured, the average NLO susceptibility, $\langle d_{eff}\rangle_{exp}$, can be estimated.[28] For phase-matchable materials

$$\langle d_{eff}\rangle_{exp} = \{7.98 \times 10^2[I^{2\omega}((NH_4)_2Te_2WO_8)/I^{2\omega}(LiNbO_3)]\}^{1/2}$$

where $I^{2\omega}(LiNbO_3) = 600 \times$ α-SiO_2. Because $I^{2\omega}((NH_4)_2Te_2WO_8) = 250 \times$ α-SiO_2, $\langle d_{eff}\rangle_{exp}((NH_4)_2Te_2WO_8) = 18.2$ pm/V. The strong SHG response is not only attributable to the individual β(M−O)'s (bond hyperpolarizabilities), but also to the asymmetric coordination environments of the WO_6 and TeO_4 polyhedra. Using a model described earlier, where the metal−oxygen bonds are treated as vectors and given specific β(M−O) values,[5,28,44] we were able to calculate a $\langle d_{eff}\rangle_{calc}$ of 34.3 pm/V for $(NH_4)_2Te_2WO_8$.

In addition to the SHG measurements, we also performed ferroelectric and pyroelectric measurements. With both of these phenomena, the individual polarizations, dipole moments, of the WO_6 and TeO_4 polyhedra as well as the bulk polarization of $(NH_4)_2Te_2WO_8$ are critical. Figure 4 shows the local and net dipole moment for the reported material. The local dipole moment for Te(1) is directed almost entirely along the $\pm c$-axis direction. Thus, most of the polarization attributable to Te(1) cancels. With Te(2) and W, we observe a net polarization along the $-b$-axis. As such, the direction of the total polarization in $(NH_4)_2Te_2WO_8$ is along the $-b$-axis (see Figure 4). Ferroelectric hysteresis measurements, polarization versus electric field, on bulk $(NH_4)_2Te_2WO_8$ indicate the material is "switchable". A spontaneous polarization of 0.19 $\mu C/cm^2$ was observed. The rather small spontaneous polarization value may be better understood by examining the local and net polarization in $(NH_4)_2Te_2WO_8$. The observed ferroelectric hysteresis implies that the net dipole moment in $(NH_4)_2Te_2WO_8$ may be switched, or reversed. This "switchability" of the macroscopic dipole moment indicates "switchability" in the individual dipole moments, that is, the polarization associated with the WO_6 and TeO_4 polyhedra. With the WO_6 octahedra, it is straightforward to envision the W^{6+} cation "reversing" its position and forming three short and three long W−O bonds on the opposite face. With the TeO_4 polyhedra, however, the situation is not as straightforward. For the polarization to switch directions, the lone-pair must "flip" to the opposite side, which would also involve a substantial rearrangement of the Te−O bonds. This is highly unlikely. Thus, the

(40) Dimitriev, Y.; Bart, J. C. J.; Dimitrov, V.; Arnaudov, M. *Z. Anorg. Allg. Chem.* **1981**, *479*, 229.
(41) Arnaudov, M.; Dimitrov, V.; Dimitriev, Y.; Markova, L. *Mater. Res. Bull.* **1982**, *17*, 1121.
(42) Szaller, Z.; Kovacs, L.; Poppl, L. *J. Solid State Chem.* **2000**, *152*, 392.
(43) Ok, K. M.; Halasyamani, P. S. *Inorg. Chem.* **2005**, *44*, 3919.
(44) Bergman, J. G.; Crane, G. R. *J. Solid State Chem.* **1975**, *12*, 172.

Table 4. Infrared and Raman Vibrations (cm^{-1}) for $(NH_4)_2Te_2WO_8$

IR (cm^{-1})				Raman (cm^{-1})			
N−H	W−O	Te−O	W−O−Te	N−H	W−O	Te−O	W−O−Te
3449	912	790	656	3044	906	790	644
	829	743			824	727	619
					551	671	
						433	
						394	

polarization reversibility is limited to the W^{6+} cation, resulting in the low spontaneous polarization value.

$(NH_4)_2Te_2WO_8$ also exhibits pyroelectric behavior. Pyroelectricity may be formally defined as the temperature dependence of the spontaneous polarization.[2,45] The pyroelectric coefficient, p, is defined as $(\partial P_s/\partial T)_{E,S}$, where P_s is the spontaneous polarization and T is the temperature. Constant electric field, E, and constant elastic stress, S, are the constraints. Whereas the former is straightforward to understand, the latter indicates the material is unclamped during the measurements and is free to thermally expand or contract. The pyroelectric coefficient may be divided into two parts, primary and secondary.[45] The primary pyroelectric coefficient is determined if the material is rigidly clamped during the measurement, whereas the secondary pyroelectric coefficient includes the additional change in polarization attributable to the volume change arising from the change in temperature. In practice, unclamped measurements give the sum of the primary and secondary coefficients. We measured the unclamped, that is, stress-free or total, pyroelectric coefficient, p, for $(NH_4)_2Te_2WO_8$. For pyroelectrics that exhibit ferroelectricity, the pyroelectric coefficient may be determined by measuring the remanent polarization, from the hysteresis loop, at a variety of temperatures. We measured the remanent polarization of $(NH_4)_2Te_2WO_8$ between room temperature and 230 °C with a constant electric field of 46 kV/cm (see Supporting Information). The pyroelectric coefficient is approximately -0.22 $\mu C/(m^2K)$ at 50 °C. The magnitude of the pyroelectric coefficient for $(NH_4)_2Te_2WO_8$ is smaller as compared to other ferroelectric pyroelectrics, for example, $BaTiO_3$ ($p = -200$ $\mu C/(m^2K)$) and $LiNbO_3$ ($p = -83$ $\mu C/(m^2K)$).[45] The smaller pyroelectric coefficient in $(NH_4)_2Te_2WO_8$ is likely attributable to its smaller spontaneous and remanent polarization.

Acknowledgment. We thank the Robert A. Welch Foundation and the Texas Center for Superconductivity for support. This work was also supported by the NSF through DMR-0652150. We also acknowledge Yushin Park and Prof. R. Advincula for assistance in obtaining the Raman spectra.

Supporting Information Available: X-ray crystallographic file in CIF format, calculated and observed X-ray diffraction pattern, thermogravimetric analysis diagram, phase-matching curve, and ferroelectric and pyroelectric data for $(NH_4)_2Te_2WO_8$ (PDF). This material is available free of charge via the Internet at http://pubs.acs.org.

CM7019334

(45) Lang, S. B.; Das-Gupta, D. K. Pyroelectricity: Fundamentals and Applications. In *Handbook of Advanced Electronic and Photonic Materials and Devices*; Nalwa, H. S., Ed.; Academic Press: San Francisco, 2001; Vol. 4, pp 1−55.